

Mathematical Modeling of the Transmission Dynamics of Monkeypox with the Impact of Quarantine and Public Enlightenment in Nigeria

Sefiu Onitilo¹ , Abiodun Ajani¹ , Deborah Daniel^{1*} , Ayobami Haruna¹ 

¹ Olabisi Onabanjo University, Department of Mathematical Sciences, 121103, Ago-Iwoye, Nigeria

Abstract

Monkeypox remains a public health concern in Nigeria, with periodic outbreaks reported. Despite efforts to control the disease, the number of reported cases continues to rise. Understanding the transmission dynamics of monkeypox and predicting its future spread can inform public health decision-making and guide the allocation of resources for control efforts. Hence, in this study, a deterministic model for the transmission dynamics of Monkeypox in the presence of quarantine and public enlightenment is presented. The model analysis involving the Disease Free Equilibrium (DFE) is established. Numerical simulations were used to better investigate the impact of quarantine and public enlightenment on human population. The results revealed that the effectiveness of the combined form of public awareness and quarantine produced more results followed by the effectiveness of public awareness alone, and then the result achieved when infected individuals were quarantined. If the measures were implemented with a greater degree of integration, there would be a significant reduction in the viral peak, thereby preventing its persistence within the human population.

Keywords: Monkeypox, Transmission Dynamics, Modelling, Quarantine, Public Enlightenment, Reproduction Number.

Cite this paper as: Sefiu O., Abiodun A., Deborah D. and Ayobami H. (2024). Mathematical Modeling of the Transmission Dynamics of Monkeypox with the Impact of Quarantine and Public Enlightenment in Nigeria, 8(1):1-17.

*Corresponding author: Deborah Daniel
E-mail: oludeboradaniel@gmail.com

Received Date: 18/08/2023
Accepted Date: 28/12/2023
© Copyright 2024 by
Bursa Technical University. Available
online at <http://jise.btu.edu.tr/>



The works published in the journal of Innovative Science and Engineering (JISE) are licensed under a Creative Commons Attribution-NonCommercial 4.0 International License.

1. Introduction

Monkeypox is an infectious illness caused by the monkeypox virus, which may affect both people and animals. The virus was first detected in Simians in the Democratic Republic of the Congo in 1958; however, it was not until 1970 that the first instance of human infection was officially documented. Subsequent to the aforementioned period, intermittent instances of outbreaks have transpired in many African nations, encompassing Cameroon, the Central African Republic, Ivory Coast, Liberia, Nigeria, Sierra Leone, and Sudan, along with some regions within the Americas and Europe. The virus exhibits endemicity in nations located in Central and West Africa, hence warranting attention as a significant public health issue, given its propensity to incite epidemics. The etiological agent of monkeypox is classified under the genus Orthopoxvirus, which encompasses other viruses such as those accountable for smallpox and vaccinia [6, 8, 9, 11, 22]. Although monkeypox is often less severe than smallpox, it may pose a significant risk to those with compromised immune systems, potentially leading to life-threatening outcomes. Monkeypox is classified as a zoonotic ailment, denoting its potential for inter-species transmission from animals to humans. The transmission of the virus mostly occurs through wild animals, including rodents, monkeys, squirrels, and primates, either via direct contact with these animals or by contact with their bodily fluids or infected animal products. Monkeypox has a variety of clinical presentations, including symptoms such as fever, headache, muscular pains, backache, enlarged lymph nodes, chills, and exhaustion. The appearance of a dermatological eruption becomes evident, often commencing in the face area and then spreading to diverse anatomical places.

The comprehensive comprehension of the natural history of the monkeypox virus remains enigmatic, requiring more inquiry to determine the specific reservoir(s) and the processes by which viral circulation is maintained in its natural habitat. One potential risk factor that has been identified in research is the consumption of undercooked meat and other animal-derived products acquired from animals that are infected [4]. In nations where the illness is non-endemic and instances have been detected, more endeavours are being undertaken within the realm of public health. These efforts include comprehensive investigations aimed at identifying patients, tracking contacts, doing laboratory analysis, managing clinical issues, and implementing isolation measures with adequate support. Genomic sequencing has been used to determine the particular viral clade(s) of monkeypox in the ongoing epidemic, if possible. Moreover, as stated in the reference [1], control techniques for respiratory illnesses include a variety of policies, such as quarantine protocols, infection control measures, identification and isolation of cases, and vaccination interventions.

The use of mathematical modeling presents a feasible methodology for examining the intricacies of infectious diseases, such as monkeypox. Mathematical models have the capacity to forecast the propagation of diseases, assess the efficacy of various intervention approaches, and provide valuable insights into the fundamental principles of disease transmission. Numerous scholars have used mathematical models to investigate the aetiology of diseases in diverse populations, and these models have shown their efficacy and utility (Malaria [15], HIV [3], Cholera [16], COVID-19 [5, 13–14, 17–18], Monkeypox [2, 6–11, 19–23]). Gaining insight into the transmission mechanisms of monkeypox and developing projections about its future dissemination might provide valuable information for public health decision-making and facilitate the effective allocation of resources towards control measures. A variety of models using different methodologies have been developed and analysed to improve comprehension of the transmission dynamics and control tactics of monkeypox.

The authors of [7] have created a deterministic mathematical model to describe the transmission dynamics of the monkeypox virus. The model includes a component representing the imperfect vaccination efficacy within the human subpopulation. The stability of the equilibrium states of the model equation was examined and obtained. A numerical simulation was conducted to emphasise the impact of several levels of immune system strength (weak, medium, and strong) on different epidemiological states. Additionally, the simulation examined the influence of infection and vaccination rates on the prevalence of the disease and the number of vulnerable individuals, respectively. The mathematical model of monkey-pox transmission was investigated by [10] using ordinary differential equations. The validity of the model's feasible area was confirmed, demonstrating the presence of positive solutions. The mathematical model of monkeypox viral transmission dynamics, including two interacting host populations, namely humans and rats, was investigated by [23]. The implementation of quarantine measures and public awareness campaigns serves as a mechanism for managing the transmission of the illness among the human population. The authors in reference [19] put out a deterministic mathematical model with the aim of examining the dynamics of the monkeypox virus among the human population. The results indicate that implementing measures to separate individuals who are infected from the broader community may effectively mitigate the spread of diseases. The researchers in this work [20] developed and analysed a deterministic mathematical model in order to investigate the dynamics of the monkeypox virus. This study establishes the conditions for determining the asymptotic stability of both disease-free and endemic equilibria, both at the local and global levels. The findings indicate that the use of strategies to separate individuals who are infected from the wider community may be an effective approach to reducing the transmission of illnesses.

Nevertheless, a dearth of comprehension persists about the determinants that propel the transmission and dissemination of the ailment within the Nigerian context. Nigeria, being the most populous nation in Africa, has a diversified population and varied topography, both of which may have a significant influence on the transmission patterns of infectious illnesses. The existence of this information gap hinders policymakers' capacity to formulate and implement effective control and preventive initiatives. Hence, it is essential to develop a mathematical model that may provide valuable insights into the transmission dynamics of monkeypox in Nigeria and facilitate informed decision-making on disease management strategies. Therefore, this study considered the rodent-human transmission route named SIQR-SEI model. This model enhances the classic SEIR and SIR framework by incorporating vaccination, transmission through rodents, quarantine phases, and unique interaction dynamics among different population groups. The process includes vaccination of individuals, a transmission route that involves interaction with infected rodents resulting in human illness, and a quarantine phase for observed individuals before recovery.

2. Material and Methods

2.1. Mathematical Formulation

The model takes into account two distinct populations, one consisting of humans and the other consisting of rodents. The human population may be classified into four distinct categories: susceptible, infected, quarantined, and recovered. The population of rodents is classified into three distinct categories, namely, susceptible, exposed, and infected.

Table 1. State Variable of the Model and their descriptions.

Variables	Description
$S_H(t)$	Susceptible human population at time (t)
$I_H(t)$	Infected human population at time (t)
$Q_H(t)$	Quarantined human population at time (t)
$R_H(t)$	Recovered human population at time (t)
$S_R(t)$	Susceptible rodent population at time (t)
$E_R(t)$	Exposed rodent population at time (t)
$I_R(t)$	Infected rodent population at time (t)

Table 2. Model parameters with their descriptions.

Parameters	Description
μ_H	Recruitment rate of human population
μ_R	Recruitment rate of rodent population
σ_1	Contact rate of rodent population
σ_2	Contact rate of human population
σ_3	Contact rate of rodent population
Φ_H	Natural death rate of human population
γ_H	Disease induced death rate of human population
ρ_H	Recovery rate of human population
η	Progression rate from infected to quarantine
Φ_R	Natural death rate of rodents population
γ_R	Disease induced death rate of rodent population
ξ	Effectiveness of quarantine and treatment
α	Effectiveness of public enlightenment and campaign

2.2. Model Assumptions

The model's derivation is based on the following assumptions: there is an absence of emigration from the overall population, and likewise, there is a lack of immigration into the population. During a certain period, a minute fraction of people experienced migration into or out of the population and subsequently received vaccination; maturation, also known as maturity, is defined as the interval between the time of infection and the onset of observable symptoms, often occurring within a timeframe of 14 to 21 days; the susceptible population is first exposed to a type of rodent that carries the infectious agent, resulting in their subsequent infection; and certain persons who have contracted the infection are sent to a designated facility where they undergo quarantine to conduct observational procedures. The process of recruiting individuals from the S_H class to the I_H class occurs via interactions with individuals from the I_R class within the rodent population. The process of recruiting individuals from the I_H class to the Q_H class occurs at a pace denoted by the symbol η . The recruitment of individuals from the Q_H class into the R_H class is contingent upon the efficacy of the quarantine and observation protocol, denoted by the rate ρ ; the occurrence of death is inherent in the model and it transpires uniformly across all classes at a constant

rate μ . However, it is worth noting that there is an increased mortality rate seen in the I_H and Q_H classes as a result of infection.

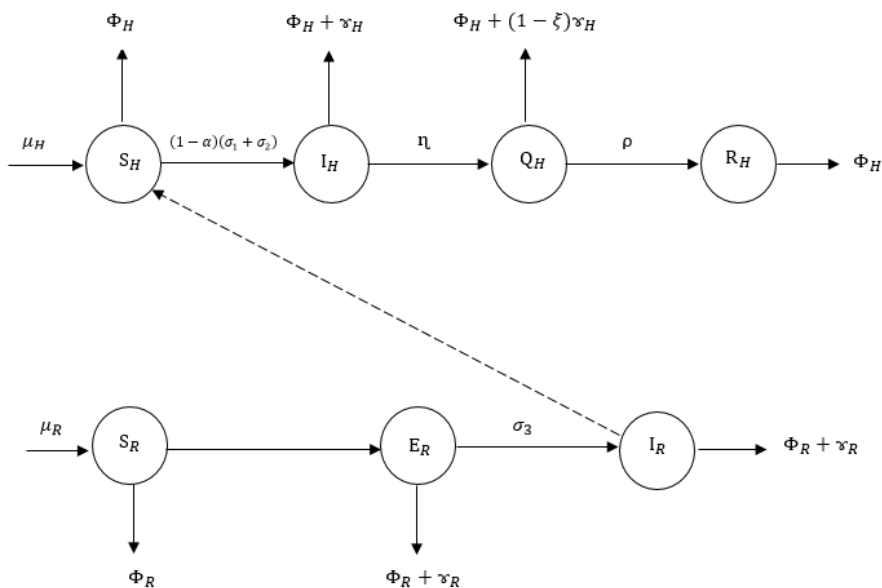


Figure 1. The flow diagram of the model.

2.3. The Model Equations

$$\frac{dS_H}{dt} = \mu_H - [(1 - \alpha)(\sigma_1 + \sigma_2)I_R - \Phi_H]S_H \tag{1}$$

$$\frac{dI_H}{dt} = (1 - \alpha)(\sigma_1 + \sigma_2)I_R S_H - [(\Phi_H + \varkappa_H) + \eta]I_H \tag{2}$$

$$\frac{dQ_H}{dt} = \eta I_H - [\Phi_H + (1 - \xi)\varkappa_H + \rho]Q_H \tag{3}$$

$$\frac{dR_H}{dt} = \rho Q_H - \Phi_H R_H \tag{4}$$

$$\frac{dS_R}{dt} = \mu_R - [\Phi_R + \sigma_3]S_R \tag{5}$$

$$\frac{dE_R}{dt} = \sigma_3 S_R - [(\Phi_R + \varkappa_R) + \sigma_3]E_R \tag{6}$$

$$\frac{dI_R}{dt} = \sigma_3 E_R - (\Phi_R + \varkappa_R)I_R \tag{7}$$

Such that

$$N_H(t) = S_H(t) + I_H(t) + Q_H(t) + R_H(t) \tag{8}$$

$$N_R(t) = S_R(t) + E_R(t) + I_R(t) \tag{9}$$

$$\frac{dN_H(t)}{dt} = \frac{dS_H(t)}{dt} + \frac{dI_H(t)}{dt} + \frac{dQ_H(t)}{dt} + \frac{dR_H(t)}{dt} \tag{10}$$

$$\frac{dN_R(t)}{dt} = \frac{dS_R(t)}{dt} + \frac{dE_R(t)}{dt} + \frac{dI_R(t)}{dt} \tag{11}$$

Such that

$$\frac{dN_H(t)}{dt} = \mu_H - [(1 - \alpha)(\sigma_1 + \sigma_2)I_R + \Phi_H]S_H + (1 - \alpha)(\sigma_1 + \sigma_2)I_R S_H - [(\Phi_H + \varkappa_H) + \eta]I_H + \eta I_H - \tag{12}$$

$$[\Phi_H + (1 - \xi)\varkappa_H + \rho]Q_H + \rho Q_H - \Phi_H R_H$$

$$\frac{dN_R(t)}{dt} = \mu_R - [\Phi_R + \sigma_3]S_R + \sigma_3 S_R - [(\Phi_R + \varkappa_R) + \sigma_3]E_R + \sigma_3 E_R - (\Phi_R + \varkappa_R)I_R \quad (13)$$

Let $S_h = \frac{S_H}{N_H}$ $I_h = \frac{I_H}{N_H}$ $Q_h = \frac{Q_H}{N_H}$ $R_h = \frac{R_H}{N_H}$ (14)

Also, $S_r = \frac{S_R}{N_R}$ $E_r = \frac{E_R}{N_R}$ $I_r = \frac{I_R}{N_R}$ (15)

Then the normalized system is as follows;

$$\frac{dS_h}{dt} = \frac{1}{N_H} \left[\frac{dS_H(t)}{dt} - S_h \frac{dN_H(t)}{dt} \right]$$

Substituting (1) and (10) using (14)

$$\frac{dS_h}{dt} = \frac{\mu_H(1-S_h)}{N_H} - (1 - \alpha)(\sigma_1 + \sigma_2)I_r S_h - \Phi_H S_h + (1 - \xi)\varkappa_H S_h q_h - I_r S_h S_h + \Phi_H S_h S_h + \Phi_H S_h I_h + \varkappa_H S_h I_h + \Phi_H S_h Q_h + \Phi_H S_h R_h \quad (16)$$

$$\frac{dI_H(t)}{dt} = \frac{1}{N_H} \left[\frac{dI_H(t)}{dt} - I_h \frac{dN_H(t)}{dt} \right]$$

$$\frac{dI_H(t)}{dt} = (1 - \alpha)(\sigma_1 + \sigma_2)I_r S_h - (\Phi_H + \varkappa_H)I_h - \eta I_h - \frac{\mu_H I_h}{N_H} + \Phi_H I_h S_h + \Phi_H I_h I_h + \varkappa_H I_h I_h - \Phi_H I_h Q_h + (1 - \xi)\varkappa_H I_h Q_h - \Phi_H I_h R_h \quad (17)$$

$$\frac{dQ_H(t)}{dt} = \frac{1}{N_H} \left[\frac{dQ_H(t)}{dt} - Q_h \frac{dN_H(t)}{dt} \right]$$

$$\frac{dQ_H(t)}{dt} = \eta I_h - \Phi_H Q_h - (1 - \xi)\varkappa_H Q_h - \rho Q_h - \frac{\mu_H Q_h}{N_H} - I_r S_h Q_h + \Phi_H Q_h S_h + \Phi_H Q_h I_h + \varkappa_H Q_h I_h + \Phi_H Q_h + (1 - \xi)\varkappa_H Q_h Q_h + \rho Q_h Q_h - \rho Q_h Q_h + \Phi_H Q_h R_h \quad (18)$$

$$\frac{dR_H(t)}{dt} = \frac{1}{N_R} \left[\frac{dR_H(t)}{dt} - R_h \frac{dN_H(t)}{dt} \right]$$

$$\frac{dR_H(t)}{dt} = \rho q_h - \Phi_H R_h - \frac{\mu_H R_h}{N_H} - I_r R_h S_h + \Phi_H R_h S_h + \Phi_H R_h R_h \quad (19)$$

$$\frac{dS_R(t)}{dt} = \frac{1}{N_R} \left[\frac{dS_R(t)}{dt} - S_r \frac{dN_R(t)}{dt} \right]$$

$$\frac{dS_R(t)}{dt} = \frac{\mu_R(1 - S_r)}{N_R} - (\Phi_R + \sigma_3)S_r + (\Phi_R + \sigma_3)S_r S_r - \sigma_3 S_r S_r + (\Phi_R + \varkappa_R)E_r S_r + \frac{(\Phi_R + \varkappa_R)S_r I_r}{N_R} \quad (20)$$

$$\frac{dE_R(t)}{dt} = \frac{1}{N_R} \left[\frac{dE_R(t)}{dt} - E_r \frac{dN_R(t)}{dt} \right]$$

$$\frac{dE_R(t)}{dt} = \sigma S_r - (\Phi_R + \varkappa_R)E_r - \sigma_3 E_r - \frac{\mu_R E_r}{N_R} + (\Phi_R + \sigma_3)E_r S_r - \sigma_3 E_r S_r + (\Phi_R + \varkappa_R)E_r E_r + (\Phi_R + \varkappa_R)E_r I_r \quad (21)$$

$$\frac{dI_R(t)}{dt} = \frac{1}{N_R} \left[\frac{dI_R(t)}{dt} - I_r \frac{dN_R(t)}{dt} \right]$$

$$\frac{dI_R(t)}{dt} = \sigma e_r - (\Phi_R + \varkappa_R)I_r - \frac{\mu_R I_r}{N_R} + (\Phi_R + \sigma_3)I_r S_r - \sigma_3 I_r S_r + (\Phi_R + \varkappa_R)E_r I_r + (\Phi_R + \varkappa_R)I_r I_r \quad (22)$$

However,

$$S_h + I_h + Q_h + R_h = 1 \quad \text{and also}$$

$$S_r + E_r + I_r = 1 \quad (23)$$

2.4. Existence and Uniqueness of Disease Free Equilibrium State E_0 of the Model

The disease free equilibrium state is both human and rodent hand side of equation (13) - (22) while setting the disease component $I_h = Q_h = R_h = 0, E_r = I_r = 0$

$$0 = \mu_H \frac{(1 - S_h)}{N_H} - S_h[(1 - \alpha)(\sigma_1 + \sigma_2) - I_r - \Phi_H - I_r S_h + \Phi_H S_h] \quad (24)$$

$$0 = (1 - \alpha)(\sigma_1 + \sigma_2)S_h \quad (25)$$

Let $\beta = (1 - \alpha)(\sigma_1 + \sigma_2)$

Hence,

$$0 = \beta S_h$$

$$S_h = 0 \quad (26)$$

Substituting (26) into (24)

$$0 = \frac{\mu_H}{N_H}$$

Hence,

$$0 = -S_h \beta + I_r S_h + \Phi_H S_h - I_r S_h^2 + \Phi_H S_h^2$$

Factorising S_h

$$0 = S_h[-\beta + I_r + \Phi_H] - S_h^2[I_r + \Phi_H]$$

Also,

$$0 = \mu_R \frac{(1 - S_r)}{N_R} - (\Phi_R + \sigma_3)S_r + (\Phi_R + \sigma_3)S_r^2 - \sigma_3 S_r^2 \quad (27)$$

$$0 = \sigma S_r - (\Phi_R + \gamma_R)E_r - \sigma_3 E_r - \frac{\mu_R E_r}{N_R} + (\Phi_R + \sigma_3)E_r S_r - \sigma_3 E_r S_r + (\Phi_R + \gamma_R)E_r E_r + (\Phi_R + \gamma_R)E_r I_r$$

$$0 = \sigma S_r \quad (28)$$

$$\text{Then } S_r = 0 \quad (29)$$

Substitute (29) into (27), we have

$$0 = \frac{\mu_R}{N_R} \quad (30)$$

2.5. The Disease Free Equilibrium

$$\text{Let } [S'_h, I'_h, Q'_h, R'_h, S'_r, E'_r, I'_r] = E_0 = [S^*_h, I^*_h, Q^*_h, R^*_h, S^*_r, E^*_r, I^*_r] \quad (31)$$

$$E_0 = \left[\frac{\mu_H}{\Phi_H}, 0, 0, 0, \frac{\mu_R}{\Phi_R}, 0, 0 \right] \quad (32)$$

$$\text{At the disease free equilibrium} \quad N_H^* = \frac{\mu_H}{\Phi_H} \quad N_R^* = \frac{\mu_R}{\Phi_R}$$

2.6. Stability Analysis of Disease Free Equilibrium State

To study the behavior of the system (16) – (22) around the disease free equilibrium state

$E_0 = \left[\frac{\mu_H}{\Phi_H}, 0, 0, 0, \frac{\mu_R}{\Phi_R}, 0, 0 \right]$, The linearized stability technique proposed in reference [17] is used, resulting in the derivation of a Jacobian transformation denoted as $J(E^0)$.

$$J(E_0) = \begin{bmatrix} -\left[\frac{\mu_H}{N_H} + (1 - \alpha)(\sigma_1 + \sigma_2) \right] & 0 & 0 & 0 & 0 & 0 & 0 \\ (1 - \alpha)(\sigma_1 + \sigma_2) & -((\Phi_H + \varkappa_H) + \eta) & 0 & 0 & 0 & 0 & 0 \\ 0 & \eta & -\rho & 0 & 0 & 0 & 0 \\ 0 & 0 & \rho & 0 & 0 & 0 & 0 \\ 0 & 0 & 0 & 0 & -\frac{\mu_R}{N_R} + (\Phi_R + \sigma_3) & 0 & 0 \\ 0 & 0 & 0 & 0 & \sigma & -((\Phi_R + \varkappa_R) + \sigma) & 0 \\ 0 & 0 & 0 & 0 & 0 & \sigma & -(\Phi_R + \varkappa_R) \end{bmatrix} \quad (33)$$

We now proceed to find the determinant of the Jacobian matrix $J E_0$. The determinant of a Jacobian matrix is given by the recursive definition for a 7 x 7 matrix.

$$Det [J(E_0)] = a_{11} \det[J(E_{0_{11}})] - a_{12} \det[J(E_{0_{12}})] + a_{13} \det[J(E_{0_{13}})] - a_{14} \det[J(E_{0_{14}})] + a_{15} \det[J(E_{0_{15}})] - a_{16} \det[J(E_{0_{16}})] + a_{17} \det[J(E_{0_{17}})]$$

From equation (33), $Det J(E_0) > 0$.

Likewise, by examining the trace of the Jacobian matrix $J[E_0]$ as shown in equation (33), it can be seen that

$$Trace J(E_0) = -\left[\frac{\mu_H}{N_H} + (1 - \alpha)(\sigma_1 + \sigma_2) \right] - [(\Phi_H + \varkappa_H) + \eta] - \rho - \left[\frac{\mu_R}{N_R} - \Phi_R + \sigma_3 \right] - [(\Phi_R + \varkappa_R) + \sigma] - (\Phi_R + \varkappa_R) \quad (34)$$

$Trace J(E_0)$ as shown above is < 0 .

Hence, $Trace J(E_0) < 0$

Since $Det [J(E_0)] > 0$ and $Trace J(E_0) < 0$ fulfill the predetermined threshold conditions according to Gerald (2012), the monkeypox virus disease free equilibrium $[E_0]$ also satisfies the requirements for a locally or globally asymptotic stability for the recovered population.

2.7. The Basic Reproductive Number (R_0) of the Model

The basic reproduction number, commonly represented as R_0 , is a fundamental measure in the field of epidemiology. The basic reproduction number (R_0) quantifies the contagiousness of a disease by indicating the average number of secondary infections induced by a single sick individual in a community that is entirely susceptible to the disease. In order to calculate the basic reproduction number (R_0) for the model (16-22), the methods outlined in reference [17] will be used, using the next generation matrix (NGM) method.

$$F = \begin{bmatrix} (1 - \alpha)\sigma_2 & (1 - \alpha)\sigma_1 \\ 0 & \sigma_3 \end{bmatrix} \quad (35)$$

$$V = \begin{bmatrix} \Phi_H + \varkappa_H + \eta & 0 \\ 0 & \Phi_R + \varkappa_R \end{bmatrix} \quad (36)$$

$$V^{-1} = \begin{bmatrix} -1 & 0 \\ \frac{1}{\Phi_H + \varkappa_H + \eta} & -1 \\ 0 & \frac{1}{\Phi_R + \varkappa_R} \end{bmatrix} \quad (37)$$

Where F represents the rate at which new infections occur and V represents the movement of persons across compartments via various ways. Then the next matrix denoted by FV^{-1} is given as

$$FV^{-1} = \begin{bmatrix} (1-\alpha)\sigma_2 & (1-\alpha)\sigma_1 \\ 0 & \sigma_3 \end{bmatrix} \begin{bmatrix} \frac{-1}{\Phi_H + \gamma_H + \eta} & 0 \\ 0 & \frac{-1}{\Phi_R + \gamma_R} \end{bmatrix} \tag{38}$$

$$FV^{-1} = \begin{bmatrix} \frac{-(1-\alpha)\sigma_2}{\Phi_H + \gamma_H + \eta} & \frac{-(1-\alpha)\sigma_1}{\Phi_R + \gamma_R} \\ 0 & \frac{-\sigma_3}{\Phi_R + \gamma_R} \end{bmatrix} \tag{39}$$

We find the Eigen values of FV^{-1} by setting the determinant $|FV^{-1} - \lambda I| = 0$, I is a unit matrix

$$\left| \begin{bmatrix} \frac{-(1-\alpha)\sigma_2}{\Phi_H + \gamma_H + \eta} & \frac{-(1-\alpha)\sigma_1}{\Phi_R + \gamma_R} \\ 0 & \frac{-\sigma_3}{\Phi_R + \gamma_R} \end{bmatrix} - \begin{bmatrix} \lambda & 0 \\ 0 & \lambda \end{bmatrix} \right| = 0 \tag{40}$$

$$\left| \begin{bmatrix} \frac{-(1-\alpha)\sigma_2}{\Phi_H + \gamma_H + \eta} - \lambda & \frac{-(1-\alpha)\sigma_1}{\Phi_R + \gamma_R} \\ 0 & \frac{-\sigma_3}{\Phi_R + \gamma_R} - \lambda \end{bmatrix} \right| = 0 \tag{41}$$

$$\left[\frac{-\sigma_3}{\Phi_R + \gamma_R} - \lambda \right] \left[\frac{-(1-\alpha)\sigma_2}{\Phi_H + \gamma_H + \eta} - \lambda \right] - 0 = 0 \tag{42}$$

From (42),

$$\frac{-\sigma}{\Phi_R + \gamma_R} = \lambda_1$$

$$\frac{-(1-\alpha)\sigma_2}{\Phi_H + \gamma_H + \eta} = \lambda_2$$

Since $\lambda_1 < 0$ and also $\lambda_2 < 0$ in which $0 < 1$, hence, $R_0 < 1$ which satisfies the threshold.

3. Results and Discussion

In this section, the effectiveness of public awareness and campaigns and the effectiveness of the infected quarantine on the spread of the monkeypox virus are examined. The numerical simulation of the monkeypox virus is analysed using the baseline values given in Table 3. The numerical simulations were done and plotted against time (months) using MATLAB, and the results are shown in Figures 2–13 to illustrate the effect of public awareness and campaigns and the effectiveness of getting the infected quarantined.

Table 3. Model parameters and values used in the simulation.

Parameters	Values	Source
μ_H	0.029	[3,21]
μ_R	0.2	[3,21]
σ_1	0.00006	[2,21]
σ_2	0.00025	[2,21]
σ_3	0.027	[2,21]
Φ_H	0.15	[2,21]
ψ_H	0.2	[12,21]
η	0.83	[3,21]
Φ_R	0.002	[2,21]
ψ_R	0.5	[21]
ρ	0.52	[21]

α	0 – 1	Control Parameter
ϵ	0 – 1	Control Parameter

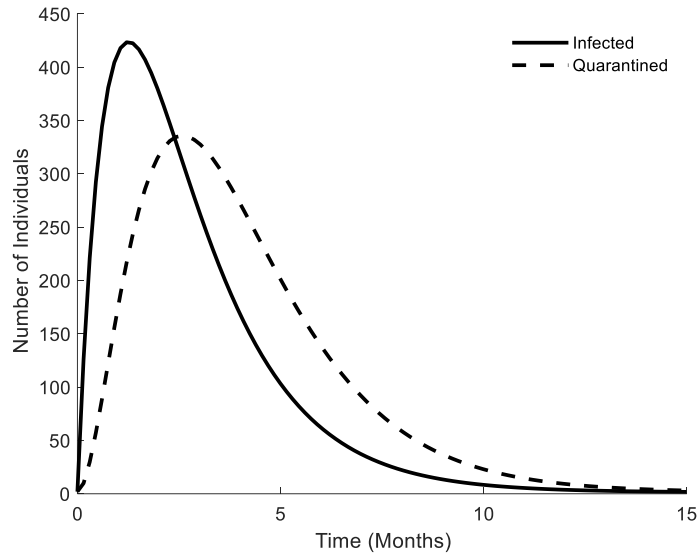


Figure 2. Numerical Simulation of the infected and quarantined population.

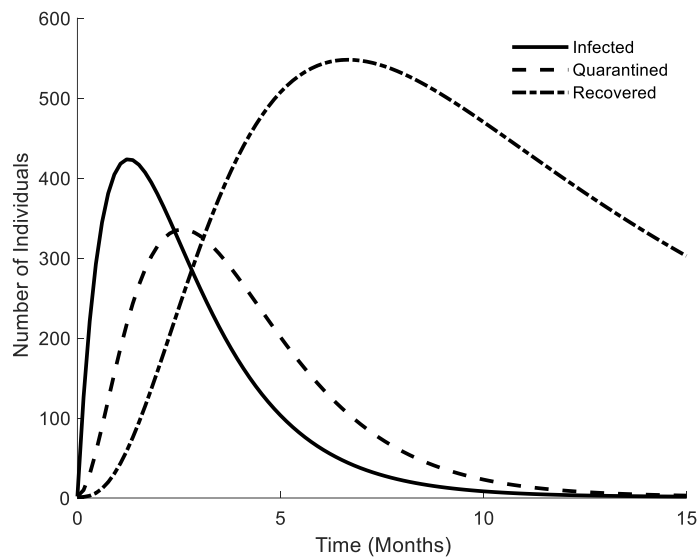


Figure 3. Numerical Simulation of the infected, quarantined and recovered population.

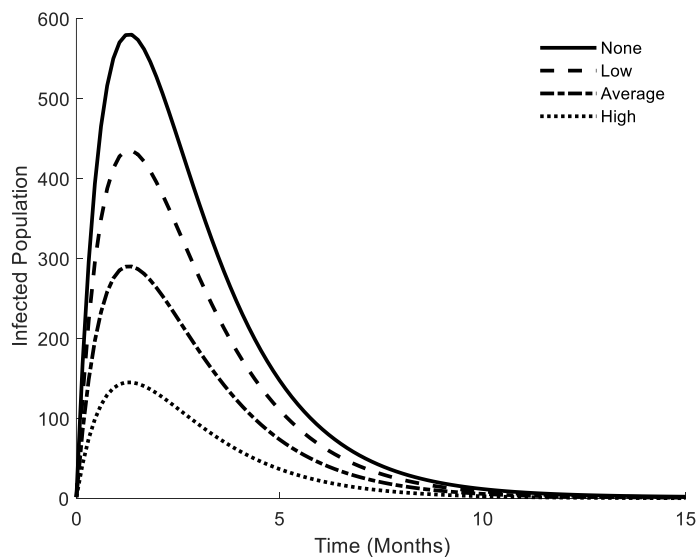


Figure 4. Variation in infected population for measuring the effectiveness of public enlightenment.

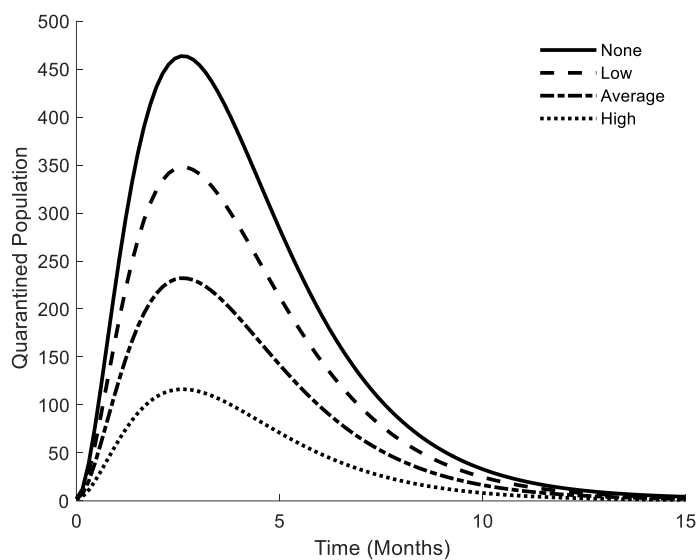


Figure 5. Variation in quarantined population for measuring the effectiveness of public enlightenment.

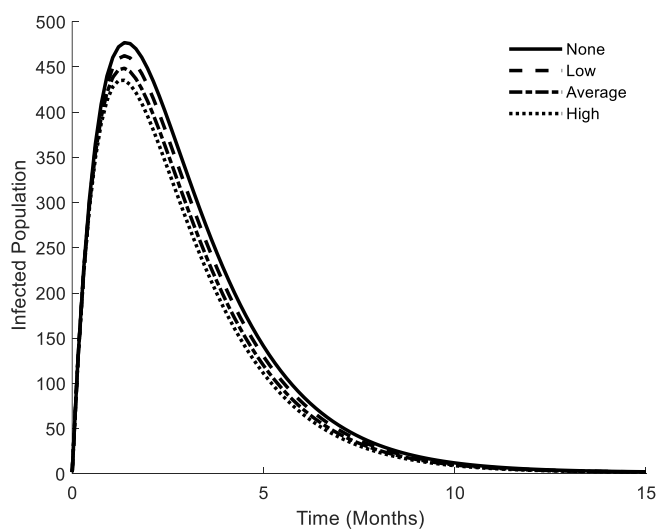


Figure 6. Variation in infected population for measuring the effectiveness of quarantined.

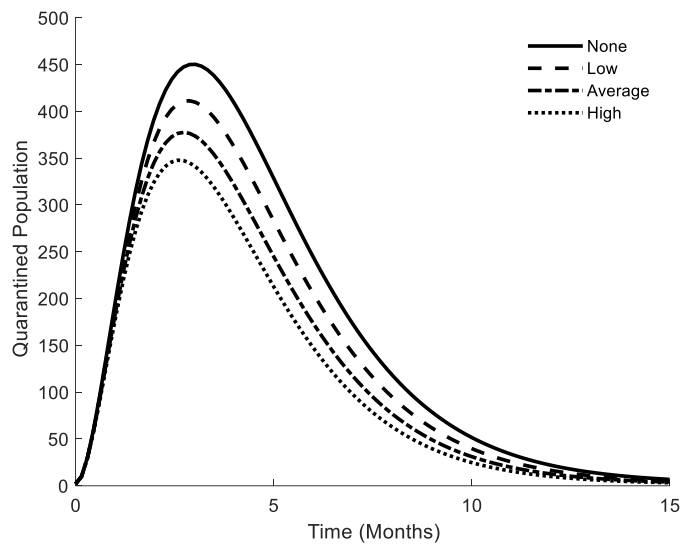


Figure 7. Variation in quarantined population for measuring the effectiveness of quarantined.

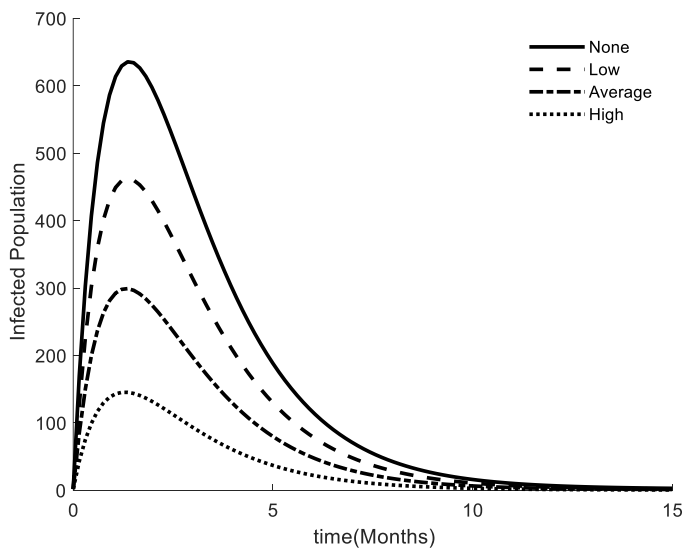


Figure 8. Variation in infected population for measuring the effectiveness of public enlightenment and rate of quarantined.

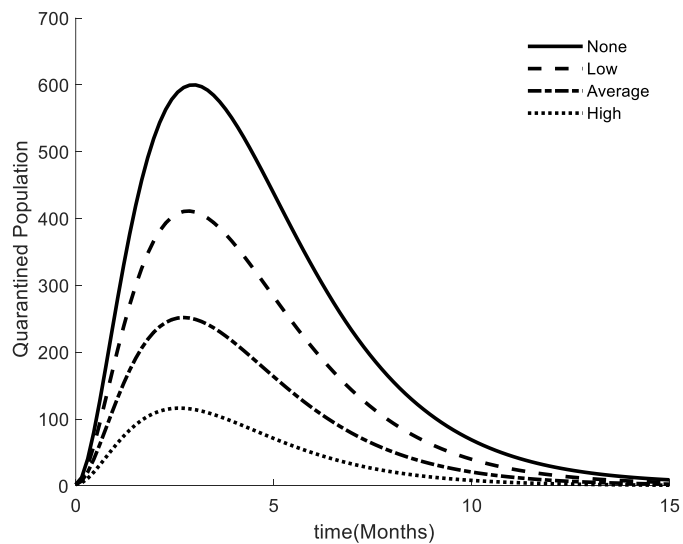


Figure 9. Variation in quarantined population for measuring the effectiveness of public enlightenment and the rate of

quarantined.

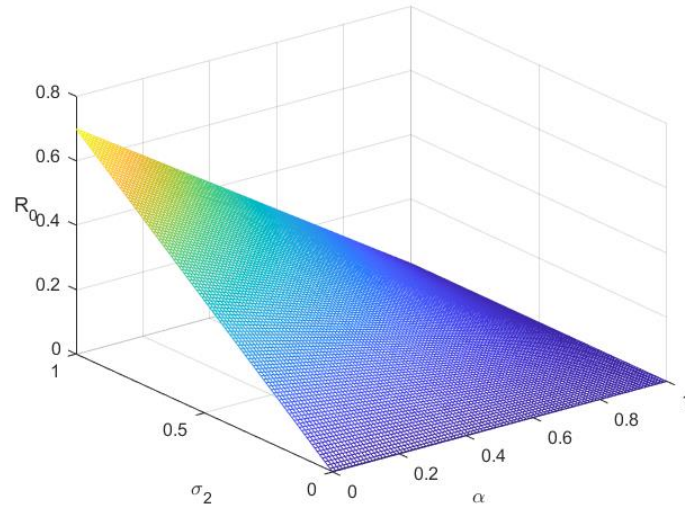


Figure 10. Surface plot showing the impact of α and σ_2 on R_0 .

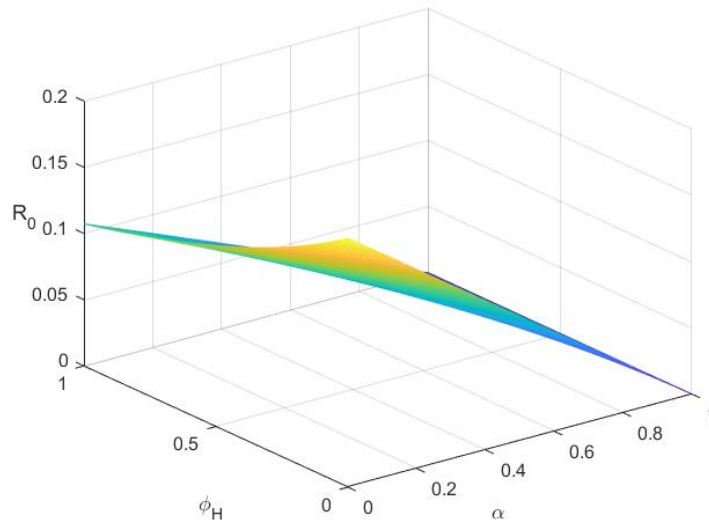


Figure 11. Surface plot showing the impact of α and ϕ_H on R_0 .

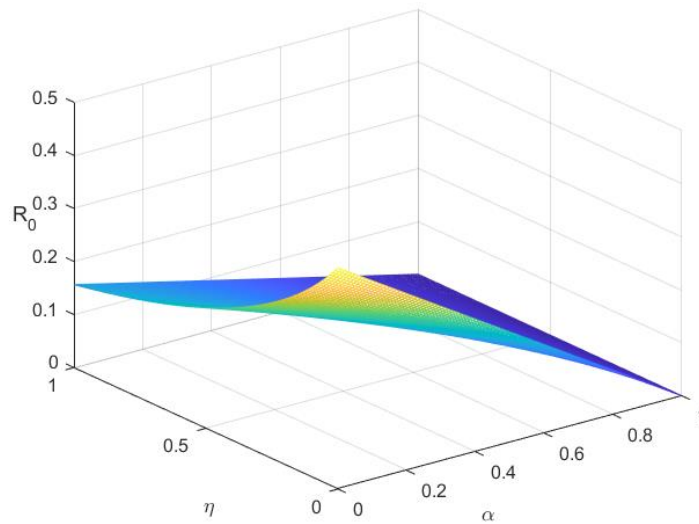


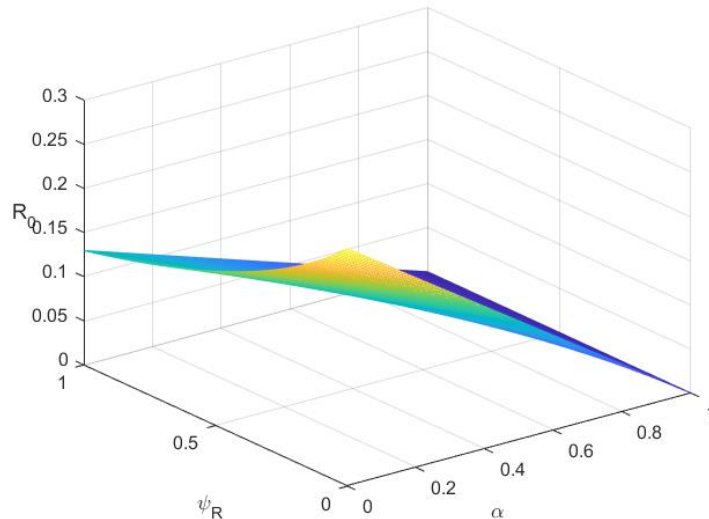
Figure 12. Surface plot showing the impact of α and η on R_0 enlightenment.**Figure 13.** Surface plot showing the impact of α and ψ_R on R_0 .

Figure 2 describes the numerical simulation of the infected and quarantined populations. The infected population is seen to have reached its peak before the quarantined population and then drastically reduced. Furthermore, the number of individuals in the infected population is seen to be higher than those in the quarantined population, which implies a high rate of infection at the start of the viruses. After a while, individuals then rush into the quarantined population owing to the different peak attained by the infected population and quarantined population. Figure 3 illustrates the numerical simulation of the infected, quarantined, and recovered populations. It is observed that as the number of individuals keeps increasing in the infected compartment and quarantined population, the population of the recovery compartment keeps increasing.

Figure 4 depicts the variation in the infected population for measuring the effectiveness of public enlightenment only. The control parameters used are: $\alpha = 0, 0.25, 0.5, 0.75$. With an increase in the parameter measuring the rate of effectiveness of public enlightenment and campaigns, the aftermath is a reduction in the infected population. This implies that if public awareness could be increased, the rate of infection would be reduced, thereby reducing the number of individuals that would be infected with monkeypox.

Figure 5 displays the variation in quarantined population for measuring the effectiveness of public enlightenment only. The control parameters used are: $\alpha = 0, 0.25, 0.5, 0.75$. It is noted that an increase in the parameter measuring the rate of effectiveness of public enlightenment and campaigns resulted in a reduction in the quarantined population. This implies that if public awareness could be increased, the rate of infection would be reduced, thereby reducing the number of individuals that would need to be quarantined with monkeypox.

Figure 6 shows the variation in the infected population for measuring the effectiveness of quarantining alone. The control parameters used are: $\epsilon = 0, 0.25, 0.5, 0.75$. As observed, with an increase in the parameter measuring the rate of effectiveness of individuals quarantined, the aftermath is a reduction in the infected population. This implies that if the number of infected populations could be increased, there would be assurance in the reduction of individuals that would be infected. However, the difference might be small, but it counts too. At least it would reduce the chances of a secondary infection of monkeypox.

Figure 7 demonstrates the variation in quarantined population for measuring the effectiveness of quarantined only. The control parameters used are: $\epsilon = 0, 0.25, 0.5, 0.75$. It is seen that the population of the quarantined compartment reduces with an increase in the rate at which individuals are quarantined.

The variation in the infected population for measuring the effectiveness of public enlightenment and the rate of quarantine is shown in Figure 8. The control parameters used are: $\alpha, \epsilon = 0, 0.25, 0.5, 0.75$. It is observed that the combined effort produces more results than the single measure. Increasing the rate of public awareness and the rate of quarantining produced greater results. This reduces the number of infections, thereby reducing the population of infected people.

The variation in quarantined population for measuring the effectiveness of public enlightenment and the rate of quarantine is described in Figure 9. The control parameters used are: $\alpha, \epsilon = 0, 0.25, 0.5, 0.75$. It is observed that the combined effort produces more results than the single measure. Increasing the rate of public awareness and the rate of quarantining produced greater results. This reduces the number of infections and, thereby, the population quarantined.

Figure 10 displays the surface plot showing the impact of α and σ_2 on R_0 . It has been found that if the rate of contact with the rodent could be reduced and the rate of awareness could be increased, then the virus would be wiped out of the human population. An increase in the contact rate of humans with a rodent would result in an increase in the reproduction number, which implies the virus would stay and the human population would soon go into extinction.

Figure 11 illustrates the surface plot showing the impact of α and ϕ_H on R_0 . Figure 11 illustrates the effectiveness of public awareness in the face of natural death. Public awareness plays a key role in reducing the reproduction number, which implies that if public awareness could be effectively imbibed, the reproduction number would reduce and stabilize.

The surface plot showing the impact of α and η on R_0 enlightenment is seen in Figure 12. It is found that if the number of infected individuals could be increased and the rate of awareness could be increased, then the virus would be wiped out in the human population.

The surface plot showing the impact of α and ψ_R on R_0 is displayed in Figure 13. It is found that if the virus death rate of rodents could be increased coupled with an increase in public awareness, the basic reproduction number would reduce drastically and the virus would be wiped out of the human population.

4. Conclusion

In this work, the dynamics of the monkeypox virus's transmission were described using a deterministic model made up of systems of ordinary differential equations. The establishment of the area in which the model is epidemiologically viable has been confirmed. The model is locally asymptotically stable when the reproduction number $R_0 < 1$, which implies that the monkeypox virus will eventually be eliminated from the population. But, unstable when $R_0 > 1$, which implies that the monkeypox virus would continue to be prevalent among us if control measures were neglected. Numerical simulations were conducted to further examine the effectiveness of public awareness and the rate at which individuals were quarantined. The study concludes that the effectiveness of the combined form of public awareness and quarantine produced more results, followed by the effectiveness of public awareness alone, and then the results achieved when infected individuals were quarantined. If the measures could

be combined at a higher rate, the virus peak would reduce greatly, and the virus would not persist among humans.

References

- [1] Babak, P., Lauren, A.M., Danuta, M.S., Mel, K., David, M.P. and Robert, C.B. (2005). Modeling Control Strategies of Respiratory Pathogens. *Emerging Infectious Diseases*, 11, 1249-1256.
- [2] Bhunu, C. P., and Mushayabasa, S. (2011). Modelling the transmission dynamics of pox-like infections. *IAENG International Journal*, 41(2):1–9.
- [3] Bhunu, C., Garira, W., and Magombedze, G. (2009). Mathematical analysis of a two strain hiv/aids model with antiretroviral treatment. *Acta Biotheoretica*, 57(3):361–381
- [4] Center for Disease Control (2022) Interim clinical guidance for the treatment of monkeypox. <https://www.cdc.gov/poxvirus/monkeypox/index.html>. Accessed 15 April 2023.
- [5] Daniel, D. O. (2020). Mathematical Model for the Transmission of Covid-19 with Nonlinear Forces of Infection and the Need for Prevention Measure in Nigeria. *Journal of Infectious Diseases and Epidemiology*, 6(5):158.
- [6] Durski, K. N. , McCollum, A. M., Nakazawa, Y., Petersen, B. W., Reynolds, M. G., Briand, S., Djingarey, M. H., Olson, V., Damon, I. K., Khalakdina, A. (2018) Emergence of monkeypox-west and central Africa, 1970–2017. *Morbidity and Mortality Weekly Report*, 67(10):306
- [7] Emeka, P., Ounorah, M., Eguda, F., Babangida, B. (2018). Mathematical model for monkeypox virus transmission dynamics. *Epidemiology: Open Access*, 8(3):1000348.
- [8] Grant, R., Nguyen, L-B. L., and Breban, R. (2020). Modelling human-to-human transmission of monkeypox. *Bulletin of the World Health Organization*, 98(9):638
- [9] Jezek, Z., Szczeniowski, M., Paluku, K., Mutombo, M., and Grab, B. (1988). Human monkeypox: confusion with chickenpox. *Acta Tropica*, 45(4):297–307.
- [10] Lasisi, N., Akinwande, N., and Oguntolu, F. (2020) Development and exploration of a mathematical model for transmission of monkeypox disease in humans. *Mathematical Models in Engineering*, 6(1):23–33
- [11] Leggiadro, R. J. (2018). Emergence of Monkeypox—West and Central Africa, 1970–2017. *Pediatric Infectious Disease Journal*, 37(7), 721–721.
- [12] Odom, M. R., Curtis, H. R, and Lefkowitz, E. J. (2009) Poxvirus protein evolution: family wide assessment of possible horizontal gene transfer events. *Virus Resolution*, 44:233–249.
- [13] Onitilo, S. A. and Daniel, D. O. (2022). Mathematical Modelling and Simulation of Coronavirus (COVID-19) in Lagos, Nigeria. *Cankaya University Journal of Science and Engineering*, 19(2):078-094.
- [14] Onitilo, S. A., Daniel, D. O. and Haruna, H. A. (2021). Modeling Analysis of Coronavirus Epidemic in Nigeria using Lyapunov functions. *FUW trends in Science and Technology Journal*, 6(2): 627-632.
- [15] Onitilo, S. A, Usman, M. A., Daniel, D. O., Odetunde, O. S., Ogunwobi, Z. O., Hamed, F. A., Olubanwo, O. O., Ajani, A. S., Sanusi, A. S., Haruna, A. H. (2022). Mathematical Modelling of the Transmission Mechanism of Plasmodium Falciparum. *Natural Sciences and Advanced Technology Education*, 31(5): 435-457.
- [16] Onitilo, S. A, Usman, M. A., Daniel, D. O., Odule, T. J., and Sanusi, A. S., (2023). Modelling the Transmission Dynamics of Cholera Disease with the Impact of Control Strategies in Nigeria. *Cankaya*

University Journal of Science and Engineering, 20(1):035-052.

- [17] Onitilo, S. A., Usman, M. A., Odetunde, S. O., Hammed, F. A., Ogunwobi, Z. O., Haruna, H. A. and Daniel, D. O. (2020a). Mathematical Modeling of 2019 Novel Coronavirus (2019 - nCoV) Pandemic and Reinfection in Nigeria using SEIAHQR model. *Bulgarian Journal of Science Education*, 29(3):398-413.
- [18] Onitilo, S. A., Usman, M. A., Taiwo, A. I. Dehinsilu, O. A., Adekola, M. A. and Daniel, D. O. (2020b). Mathematical modeling, prediction and control of COVID-19 in Nigeria as one of the Epicentre in Africa. *Africa Journal of Science and Nature*, 11:169-182. P-ISSN:2536-6904, E-ISSN: 2705-2761.
- [19] Peter, O. J., Kumar, S., Kumari, N., Oguntolu, F. A., Oshinubi, K., and Musa, R. (2021a) Transmission dynamics of monkeypox virus: a mathematical modelling approach. *Modeling Earth Systems and Environment*, 1–12
- [20] Peter, O. J., Kumar, S., Kumari, N., Oguntolu, F. A., Oshinubi, K., & Musa, R. (2021b). transmission dynamics of Monkeypox virus: a mathematical modelling approach. *Modeling Earth Systems and Environment*, 8(3), 3423–3434. <https://doi.org/10.1007/s40808-021-01313-2>
- [21] Peter, O. J., Kumar, S., Kumari, N., Oguntolu, F. A., Oshinubi, K., and Musa, R. (2022). Transmission dynamics of Monkeypox virus: a mathematical modelling approach. *Modeling Earth Systems and Environment*, 8:3423–3434.
- [22] Rezza, G. (2019). Emergence of human monkeypox in west Africa. *The Lancet Infectious Diseases*, 19(8), 797–799. [https://doi.org/10.1016/s1473-3099\(19\)30281-6](https://doi.org/10.1016/s1473-3099(19)30281-6)
- [23] Somma, S., Akinwande, N., Chado, U. (2019) A mathematical model of monkey pox virus transmission dynamics. *Ife Journal of Science*, 21(1):195–204.